Detection of Avidin Based on Rugate-structured Porous Silicon Interferometer†

Youngdae Koh, Sung Jin Kim, Jaehyun Park, Cheolyoung Park. Sungdong Cho, Hee-Gweon Woo,‡ Young Chun Ko,§,* and Honglae Sohn*

*Department of Chemistry, Chosun University, Gwangju 501-759, Korea. *E-mail:hsohn@chosun.ac.kr*
‡Department of Chemistry, Chonnam National University, Gwangju 500-757, Korea
§Department of Nano-Chemical/Environmental Engineering, Daebul University, Chonnam 526-702, Korea
**E-mail: ycko@mail.daebul.ac.kr*
Received July 12, 2007

Biosensor based on rugate PSi interferometer for the detection of avidin has been described. Rugate PSi fabricated by applying a computer-generated pseudo-sinusoidal current waveform has been prepared for the application as a label-free biosensor based on porous silicon interferometer. The fabrication, optical characterization, and surface derivatization of a rugate PSi has been described. The method to fabricate biotin-derivatized rugate PSi has been investigated. The surface and cross sectional morphology of rugate PSi are obtained with SEM. FT-IR spectroscopy is used to characterize the oxidation and functionalization reaction of rugate PSi sample. Binding of the avidin into the biotin-derivatized rugate PSi induces a change in refractive index. A red-shift of reflectivity by 18 nm in the reflectivity spectrum is observed, when the biotin-modified rugate PSi was exposed to a flow of avidin.

Key Words : Rugate structure, Porous silicon, Biotin, Avidin

Introduction

Since the discovery of porous silicon (PSi),[1] PSi has been intensively investigated for a variety of applications such as chemical[2] and biological sensors,[3] medical diagnostics,[4] optical band pass filters,[5] micro chemical reactors,[6] and micro fuel cells.[7] Recently, optical devices based on multi-structured PSi attract a great attention of the scientists. From a conceptual point of view, the former is based on optically thin and homogeneous mono-layered PSi and the latter is based on discrete multi-layered PSi structure. The direction of pores and pore diameters depend on surface orientation, doping level and type, temperature, the current density, and the composition of the etching solution.[8,9] Distributed Bragg reflector porous silicon (DBR PSi) as multi-layered PSi has been developed and typically prepared by applying a square current waveform to the etch cell. DBR PSi results in two discrete indices and exhibits photonic structure of Bragg filters.[10] Rugate-structured porous silicon having photonic structure of rugate filter in which refractive index varies sinusoidally has been recently developed by applying a computer-generated pseudo-sinusoidal current waveform.[11] Chemical modification of PSi multilayer exhibits the modification of its physical, chemical, and electronic properties. Chemical or bio molecule can be detected based on changes in the spectral interference pattern.[12,13] The rugate PSi with reflection peaks in visible spectral range was recently demonstrated to be applied for the detection of different chemical species.[14-16]

For applications in high throughput drug discovery and disease diagnostics, label-free biosensors would be important due to the advantage of easy sample preparation.[17,18] Two main optical transduction methods for label-free biosensors are both optical interferometric methods based on interferometers,[19] evanescent wave devices,[20] and grating couplers,[21] and surface plasmon methods based on metal films[22] and colloids.[23] Biosensor based on porous silicon interferometer has a great advantage due to a large surface area matrix for immobilization of a variety of biomolecules such as enzymes,[24] protein,[25] and DNA fragments.[26] Sailor *et al.* recently reported that the electronic or optical properties of mono-layered PSi can also be used as the transducer of biomolecular interaction in biosensor application.[27,28] In the present work, we have prepared biosensor based on rugate PSi interferometer. The fabrication, optical characterization, and surface derivatization of a rugate PSi are reported. For the application as a label-free biosensor, the binding interaction with avidin has been investigated.

Experimental

Preparation of Rugate PSi Samples. Heavily doped p-type silicon wafers (B-doped, orientation<100>, Siltronix, Inc.) with a resistivity in the range 0.8-0.12 mΩ·cm were used to fabricate rugate PSi by an anodic etch in ethanolic HF consisted of a 3:1 volume mixture of aqueous 48% hydrofluoric acid (ACS reagent, Aldrich Chemicals) and absolute ethanol (ACS reagent, Aldrich Chemicals). Prior to etching procedure, the silicon wafer were rinsed thoroughly with ethanol and dried under a steam of nitrogen. The galvanostatic etch was carried out in a Teflon cell by using a two-electrode configuration with a Pt mesh counter electrode. A sinusoidal current density waveform varying between 150 and 250 mA/cm^2 with 0.44 Hz was applied. The

†This paper is dedicated to Professor Sang Chul Shim on the occasion of his honorable retirement.

anodization current was supplied by a Keithley 2420 high-precision constant current source controlled by a computer to allow the formation of PSi multilayers. To prevent the photogeneration of carriers, was performed the anodization in the dark. After etching, the samples are rinsed with pure ethanol and dried with nitrogen gas.

Thermal Oxiadation of Rugate PSi. The silicon surface was predominant hydride-terminated after the etching procedure. This surface was sensitive to oxidation and hydrolysis upon exposure to aqueous solution. Thermally oxidized porous silicon samples were obtained by heat treatment in a furnace (Thermolyne F6270-26 furnace equipped with controller) using the following parameters: initial ramp rate, 5 °C/min to 300 °C; hold time, 3 h; and passive cooling to ambient temperature.

Functionalization of Oxidized Rugate PSi. The oxidized porous silicon sample and 1 mL of (3-aminopropyl)trimethoxysilane (99%, Aldrich Chemicals) were refluxed for 19 h. After functionalization with amine group, the sample was rinsed successively with toluene, acetone, and ethanol and subsequently dried under a stream of nitrogen. The 100 mg of biotin (Sigma) was dissolved in 100 mL of methylene chloride. The mixture solution was stirred vigorously for 30 min, and 1-(3-(dimethyl-amino)propyl)-3-ethylcarbodiimide hydro-chloride, EDC, (200 mg, 1 mmol) was added to the solution. The reaction mixture was allowed to stir at room temperature for 1 h. The resulting solution was added to the functionalized porous silicon chip and sample was incubated overnight. Afterward, the chip was ultra-sonicated for 3 min, washed 3 times with toluene, methylene chloride, and phosphate-buffered solution (PBS, pH = 7.4), and dried under an atmosphere.

Synthesis of 2-Pyridyl-2-carboxyethyl Disulfide. 2,2'-Bipyridyl disulfide (1 g, 4.54 mmol) was dissolved in 15 mL of ethanol (99.5%), and 0.4 mL of glacial acetic acid was added. The solution was vigorously stirred and 0.24 g (2.27 mmol) of 3-mercaptopropionic acid in 5 mL of ethanol was added by dropwise. The reaction mixture was allowed to stir at room temperature for 12 h. Removable liquid was then removed under reduced pressure. The resulting oily product mixture was dissolved in 3 mL of hexane/ether (8:2, v/v). The product was purified by silica gel column chromatography. The pyridine-2-thione eluted as a yellow band. The desired product remained on the top of the silica gel column. A few milliliters of glacial acetic acid (10 mL/250 mL of methylene chloride/ ethanol eluent) were added to the eluent mixture. The desired product (2-pyridyl-2-carboxyethyl disulfide) was collected, and the solvent was removed by evaporation. The residual acetic acid was removed under high vacuum. Isolated yield = 0.4 g (82.2%, based on 0.24 g of the 3-mercaptopropionic acid starting material).

Surface Modification of (3-Aminopropyl)trimethoxysilane Terminated Rugate PSi with 2-Pyridyl-2-carboxyethyl Disulfide. The isolated product (2-pyridyl-2-carboxyethyl disulfide, 0.2 g, 94.7 mmol) was quickly dissolved in a 10 mL of methylene chloride solution. 1-(3-(dimethylamino)propyl)-3-ethylcarbodiimide hydrochloride (EDC) (100 mg, 0.6 mmol) was added to the solution. The resulting solution was allowed to stir in dry argon gas for 30 min, before funtionalization of oxidizied rugate PSi was added. The reaction mixture was stirred for 12 h at room temperature. Afterward, the chip was washed by ethanol, methylene chloride, and acetone and then dried under an atmosphere.

Data Acquisition. Interferometric reflectance spectra of rugate PSi were recorded by using an Ocean Optics S2000 spectrometer fitted with a bifurcated fiber optic probe. A tungsten light source was focused onto the center of a porous silicon surface with a spot size of approximately 1-2 mm. Spectra were recorded with a CCD detector in the wavelength rang 400-1200 nm. The illumination of the surface as well as the detection of the reflected light was performed along an axis coincident with the surface normal.

Instrumentation. FT-IR spectra were acquired with a Nicolet model 5700 FT-IR instrument in the diffuse reflectance mode (Spectra-Tech diffuse reflectance attachment), with diffuse reflectance absorption spectra are reported in absorbance units. The morphology of rugate PSi film and polymer replica were observed with cold field emission scanning electron microscope (FE-SEM, S-4700, Hitachi). 2-Thiopyridone releases were measured by UV-vis spectrometer (UV-2401 PC, Shimazu). The quantity of 2-thiopyridone release from the functionalized rugate PSi was measured at the fixed absorption wavelength of 343 nm on a time scale.

Results and Discussion

Multilayered rugate PSi prepared by applying a computer-generated pseudo-sinusoidal current waveform exhibits high reflectivity in a specific narrow spectral region. This reflectivity can be tuned to appear anywhere in the visible to near-infrared spectral range, depending on the programmed etch waveform. Rugate filters possess a sinusoidally varying porosity gradient in the direction perpendicular to the plane of the filter. The waveform used in the present work involves a sine component, which is represented by

$$Y = \mathrm{A}\cdot\sin(kt) + B$$

where Y represents a temporal sine wave of amplitude A, frequency k, time t, and an applied current density B.

For mono-layered PSi, an anodic etch of p-type silicon wafer with resistivities of 0.1-10 Ω·cm in ethanolic HF solution generally produces PSi single layer with a network of micropores (diameter, d < 2 nm), rather than meso-(d = 2-50 nm) or macropores (d > 50 nm). The shape, size, and orientation of pores of PSi layers depend on surface orientation and the dopant level of the crystalline silicon substrate as well as the applied current density, the temperature, and the concentration of the HF etching solution. The pore size of p-type PSi can be increased by increasing the concentration of the dopant and decreasing the aqueous HF concentration. High current densities result in the desired well-defined cylindrical macropores, rather than the random

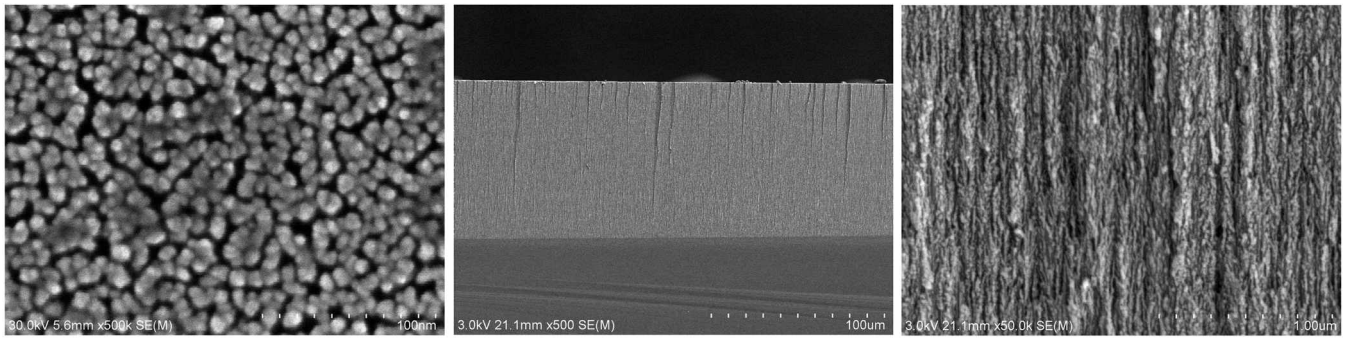

Figure 1. Surface and cross-section SEM image of prepared rugate PSi.

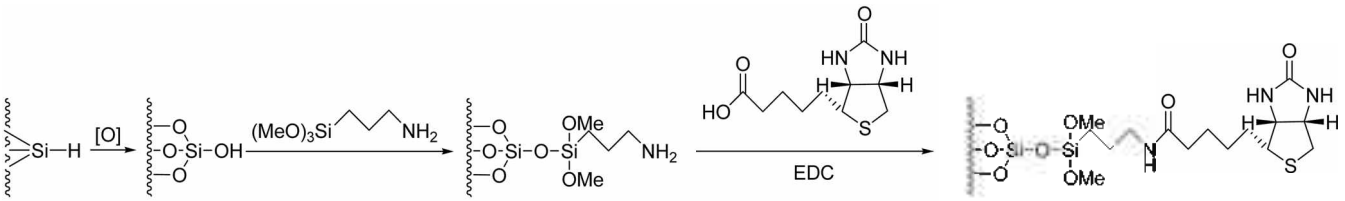

Scheme 1

orientation of highly interconnected micropores. The fabrication of macropores with diameters in the range 25-100 nm by anodizing heavily doped p-type silicon with a resistivity of 10^{-3} mΩ·cm in 25% ethanolic HF solution was reported by Herino *et al.*[29] In this work, rugate PSi with mesopores has been successfully fabricated by using a periodic galvanostatic electrochemical etch of heavily doped p-type silicon wafer with a resistivity in the range 0.8-0.12 mΩ·cm. The value of *A* and *B* was 100 and 150 mA, respectively. The surface and cross sectional morphology of rugate PSi are obtained with cold FE-SEM and shown in Figure 1. FE-SEM image of rugate PSi indicates that the prepared rugate PSi has cylindrical mesopores with the average pore size of 10 nm, which could be suitable for the detection of avidin due to its size of 56 × 50 × 40 Å.[30]

The rugate PSi displays a very sharp line in the optical reflectivity spectrum shown in Figure 2. Prepared rugate PSi exhibits a high reflectivity at 629 nm. The spectral band of the rugate film has a full-width at half-maximum (FWHM) of 15 nm, whereas the narrowest quantum dot spectrum reported at this wavelength has a FWHM of 20 nm.[31] One of the most unique features of rugate PSi is that its reflective spectral band is much narrower than the fluorescence spectrum obtained from an organic dye or core-shell quantum dot. Thus, more spectral lines can be placed in a narrower spectral window with the photonic structures.

The chemistry of functionalization is outlined in Scheme 1. The thermal oxidation of rugate PSi at 300 °C converts the hydride-terminated surface into hydroxyl terminated rugate PSi. Diffuse reflectance FT-IR spectroscopy was used to monitor the oxidation and functionalization reaction of rugate PSi sample. Figure 3A shows that the FT-IR spectrum of rugate PSi layer immediately after anodization of the silicon wafer displays a characteristic broad band centered at 2119 and 914 cm^{-1} for the υ(Si-H) stretching vibration and

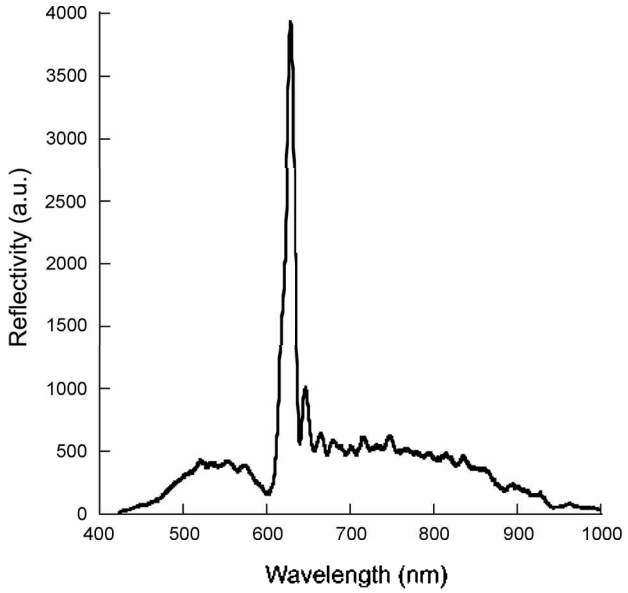

Figure 2. Optical reflectivity spectrum of rugate PSi.

δ(Si-H) bending vibration. Heavily oxidized rugate PSi samples are prepared by heating freshly etched rugate PSi in pure O_2 at 300 °C for 3 h. After the thermal oxidation of rugate PSi film, the presence of silicon oxide has been determined by FT-IR measurement as shown in Figure 3B. Thermal oxidation of the porous silicon layer results significant loss of intensity of the υ(Si-H) modes in the infrared spectrum at 2085-2150 cm^{-1}, but vibrational bands due to oxygen-back-bonded silicon hydride, υ(OSi-H) and δ(OSi-H) modes, grow at 2200-2250 and 877 cm^{-1}, respectively. Multiple silicon oxide species, Si-O-Si, display a strong, very broad absorption band between 1000 and 1200 cm^{-1}. Although we cannot quantify the coverage levels of Si-H and Si-OH on an absolute scale, the areas of the

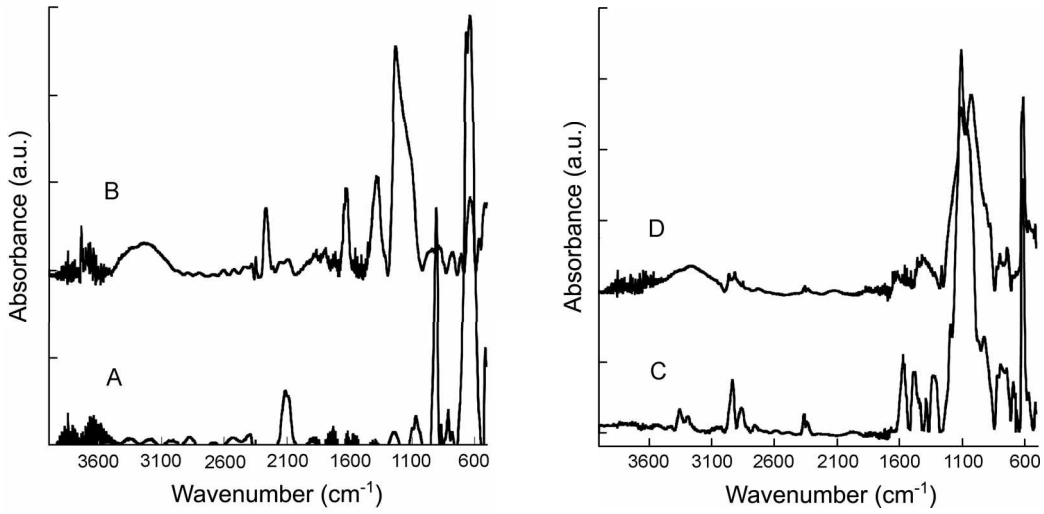

Figure 3. Diffuse reflectance FT-IR spectra of (A) a freshly etched p-type rugate PSi, (B) the wafer after 3 h oxidation with thermal, (C) the wafer after functionalization of the rugate PSi layer with (3-aminopropyl)trimethoxysilane, and (D) the wafer subsequent reaction of the surface with biotin.

infrared absorption bands provide a measure of the relative coverages on the Si-O, Si-H, and Si-OH. The relative areas of the aborption bands indicate that the oxidized rugate PSi samples contain the most O and the least H, while the fresh rugate PSi samples contain more silicon hydride species and less silicon oxide species on their surfaces. In a separate experiment, the areas of the υ(Si-H), υ(OSi-H), υ(Si-O), and υ(Si-OH) bands for the rugate PSi in the infrared spectrum were measured *in situ* during thermal oxidation (Figure 4). There is an asymptotic increase in the Si-O or OSi-H bands and a decrease in the Si-H bands over time. The thermal oxidation of rugate PSi film results the reflectivity at 556 nm shifted to shorter wavelengths by 73 nm due to the decrease of refractive index of silicon dioxide from silicon.

Condensation of the Si-OH surface of rugate PSi with (3-aminopropyl)trimethoxysilane generates a surface-bound amino group. The FT-IR spectrum shown in Figure 3C displays additional bands characteristic of the linker (the amide band of υ(N-H) at 3386 cm^{-1} and δ(N-H) at 1575 cm^{-1} and the aliphatic υ(C-H) stretching bands at 2850, 2923, and 2952 cm^{-1}). Surface derivatization leads to complete disappearance of the OSi-H vibrational bands.

To determine the surface coverage of the immobilized aminosilane linker, the functionalized surface was reduced by dithiothreitol (DTT) as shown in Scheme 2. The released 2-thiopyridone was quantified by UV/vis spectroscopy (λ_{max} = 343 nm, ε = 8.08 × 10^3 $M^{-1}cm^{-1}$).[32] The number of receptor molecules in the case of a silicon chip etched at 250-150 mA/cm^2 was in the range 300 $nmol/cm^2$, which corresponds to a surface coverage of 30-80% approximately. This calculation is based on the following parameters, assuming cylindrical pores: pore radius, 10 nm; thickness of the porous layer, 90 μm; porosity, 74%; area per molecule of the biotin linker, 0.07 $Å^2$; area of the chip, 1.2 cm^2.

The subsequent reaction with biotin as shown in Scheme 1

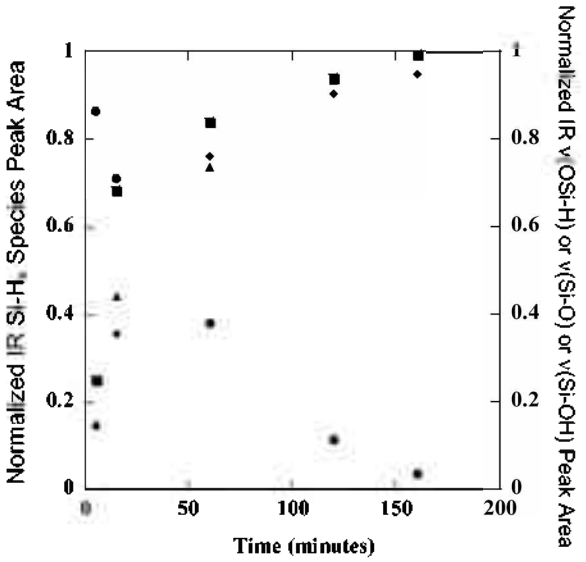

Figure 4. Normalized areas of the υ(Si-H) (●), υ(OSi-H) (◆), υ(Si-O) (■), and υ(Si-OH) (▲) bands in the infrared spectrum as a function of thermal oxidation time. Areas of the υ(Si-H) were normalized by dividing by the area of the peaks at t = 0. Areas of the υ(OSi-H), υ(Si-O), and υ(Si-OH) peaks were normalized by dividing by the area of the respective peaks measured at t = 3 h.

led to the desired biotin-funtionalized surface which was used in the avidin-binding studies (Figure 3D). The band at 1652 cm^{-1} is assigned to the carbonyl stretching vibration of the biotin head group.

The surface functionalized rugate PSi was placed in the flow cell. Aqueous PBS buffer solution was flushed to perform an initial measurement of reflectivity. The surface was rinsed thoroughly with PBS buffer solution to ensure covalent attachment to the surface and to check stability of the reflectivity measurement. The cell was then flushed with a constant flow rate of 0.8 mL/min of PBS buffer solution containing avidin (20 μM), which couples to the biotin-

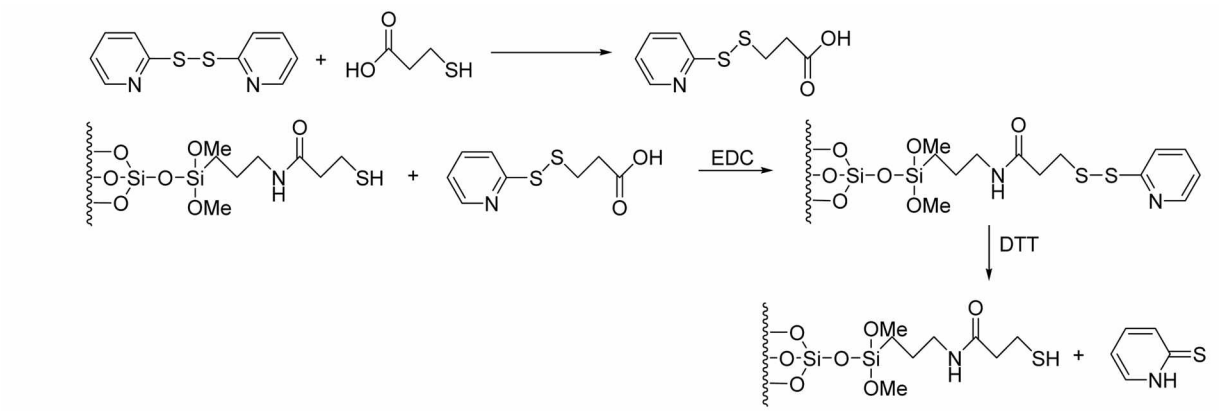

Scheme 2

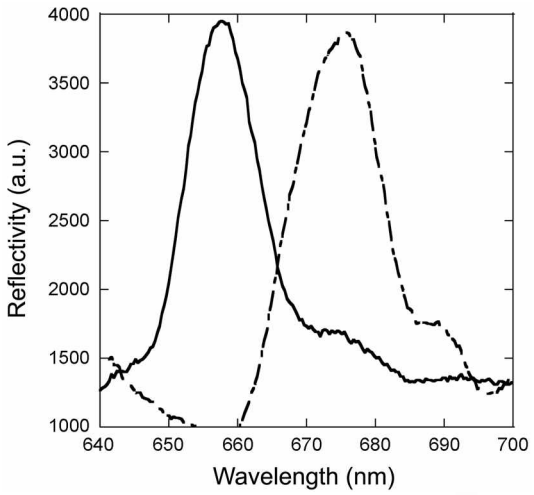

Figure 5. Optical reflectivity spectra of biotin-functionalized rugate PSi sample before (solid) and after (dashed) exposure of avidin.

modified rugate PSi surface.

Figure 4 shows the change of reflection spectrum under the exposure of avidin to the biotin-functionalized rugate PSi chip. An increase of the reflection wavelength in the reflectivity spectrum by 18 nm was observed, indicative of a change in refractive index induced by binding of the avidin into the biotin-derivatized rugate PSi film. This increase is attributed to the replacement of some of the aqueous phase with avidin. The replacement will change the mean refractive index of the rugate film and be observed as an increase of the reflection wavelength in reflectivity.

Conclusions

Rugate PSi fabricated by applying a computer-generated pseudo-sinusoidal current waveform has been prepared for the application as a label-free biosensor based on porous silicon interferometer. Prepared rugate PSi exhibits a high reflectivity with a sharp spectral line. The mean of construction of molecular architectures on rugate PSi surfaces has been investigated for the binding interaction with avidin. Diffuse reflectance FT-IR spectroscopy was used to monitor the chemical and optical characterization of rugate PSi films during step-by-step functionalzation of rugate PSi surface. The reflection spectra of biotin-modified rugate PSi was used in the avidin-binding studies. When the PBS buffer solution containing avidin was flushed into the biotin-functionalized rugate PSi chip the cell, a red-shift of reflectivity by 18 nm in the reflectivity spectrum indicates the binding of the avidin into the biotin-derivatized rugate PSi film. The red-shift results from a change in average refractive indices attributed to the replacement of some of the aqueous phase with avidin.

References and Notes

1. Uhlir, A. *Bell System Tech. J.* **1956**, *35*, 333.
2. Sohn, H.; Letant, S.; Sailor, M. J.; Trogler, W. C. *J. Am. Chem. Soc.* **2000**, *122*, 5399.
3. Lin, V. S.; Motesharei, K.; Dancil, K. S.; Sailor, M. J.; Ghadiri, M. R. *Science* **1997**, *278*, 840.
4. Simion, M.; Kleps, I.; Neghina, T.; Angelescu, A.; Miu, M.; Bragaru, A.; Danila, M.; Condac, E.; Costache, M.; Savu, L. *J. Alloy Compd.* **2007**, *434*, 830.
5. Ilyas, S.; Bocking, T.; Kilian, K.; Reece, P. J.; Gooding, J.; Gaus, K.; Gal, M. *Opt. Mater.* **2007**, *29*, 619.
6. Khan, M. A.; Haque, M. S.; Naseem, H. A.; Brown, W. D.; Malshe, A. P. *Thin Solid Films* **1998**, *332*, 93.
7. Letant, S. E.; Content, S.; Tan, T. T.; Zenhausern, F.; Sailor, M. J. *Sensor Actuat. B- Chem.* **2000**, *69*, 193.
8. Smith, R. L.; Collins, S. D. J. *Appl. Phys.* **1992**, *71*, R1.
9. Searson, P. C. *Advances in Electrochemical Sciences and Engineering*; VCH; Mannheim, Germany, 1994; p 69.
10. Lee, B. J.; Jang, S.; Sohn, H. *Solid State Phenom.* **2007**, *124-126*, 491.
11. Park, J.; Cho, S.; Ko, Y. C.; Sohn, H. *J. Korean Phys. Soc.* **2007**, *50*, 695.
12. Janshoff, A.; Dancil, K.-P. S.; Steinem, C.; Greiner, D. P.; Lin, V. S.-Y.; Gurtner, C.; Motesharei, K.; Sailor, M. J.; Ghadiri, M. R. *J. Am. Chem. Soc.* **1998**, *120*, 12108.
13. Lee, B. J.; Kim, S. G.; Sohn, H. *Key Eng. Mater.* **2006**, *321-323*, 53.
14. Li, Y. Y.; Cunin, F.; Link, J. T.; Gao, T.; Betts, R. E.; Reiver, S. H.; Chin, V.; Bhatia, S. N.; Sailor, M. J. *Science* **2003**, *199*, 11264.
15. Schmedake, T. A.; Cunin, F.; Link, J. R.; Sailor, M. J. *Adv. Mater.* **2002**, *14*, 1270.
16. Meade, S. O.; Yoon, M. S.; Ahn, K. H.; Sailor, M. J. *Adv. Mater.* **2004**, *16*, 2811.
17. Brecht, A.; Gauglitz, G. *Sensor. Actuat. B-Chem.* **1997**, *38*, 1.

18. Janata, J.; Josowicz, M.; Devaney, D. M. *Anal. Chem.* **1994**, *66*, 207R.
19. Piechler, J.; Brandenburg, A.; Brecht, A.; Wagner, E.; Gauglitz, G. *Appl. Opt.* **1997**, *36*, 6554.
20. Abel, A. P.; Weller, M. G.; Duveneck, G. L.; Ehart, M.; Widmer, H. M. *Anal. Chem.* **1996**, *68*, 2905.
21. Polzius, R.; Diessel, E.; Bier, F. F.; Bilitewski, U. *Anal. Biochem.* **1997**, *248*, 269.
22. Homola, J.; Yee, S. S.; Gauglitz, G. *Sensor. Actuat. B-Chem.* **1999**, *54*, 3.
23. Nikitin, P. I.; Beloglazov, A. A.; Kochregin, V. E.; Valeiko, M. V.; Ksenevich, T. I. *Sensor. Actuat. B-Chem.* **1999**, *54*, 43.
24. Drott, J.; Lindstrom, K.; Rosengren, L.; Laurell, T. J. *Micromech. Microeng.* **1997**, *7*, 14.
25. Laurell, T.; Drott, J.; Rosengern, L.; Lindstrom, K. *Sensor. Actuat. B-Chem.* **1996**, *31*, 161.
26. Beattie, K. L.; Beattie, W. G.; Mengm, L.; Turner, S. L.; Coral-Vazquez, R.; Sith, D. D.; McIntyre, P. M.; Dao, D. D. *Clin. Chem.* **1995**, *41*, 700.
27. Lin, V. S.-Y.; Motesharei, K.; Dancil, K.-P. S.; Sailor, M. J.; Ghadiri, M. R. *Science* **1997**, *278*, 840.
28. Sailor, M. J. *Properties of Porous Silicon*, Datareview Ser. NO. 18; Canham: London; 1997; pp 364-370.
29. Hérino, R. *Properties of Porous Silicon*, Datareview Ser. NO. 18; Canham: London, 1997; pp 89-96.
30. Pugliese, A.; Coda, A.; Malcovati, M.; Bolognesi, M. *J. Mol. Biol.* **1993**, *231*, 698.
31. Bruchez, M.; Moronne, M.; Gin, P.; Weiss, S.; Alivisatos, A. P. *Science* **1998**, *281*, 2013.
32. Stuchbury, T.; Shipton, M.; Norris, R.; Malthouse, J. P. G.; Brocklehurst, K.; Herbert, J. A. L.; Suschitzky, H. *Biochem. J.* **1975**, *151*, 417.